Faster vortex core switching with lower current density using three-nanocontact spin-polarized currents in a confined structure*

Hua-Nan Li(李化南), Zhong Hua(华中)†, and Dong-Fei Li(李东飞)

College of Physics, Jilin Normal University, Siping 136000, *China*

(Received 31 July 2016; revised manuscript received 25 September 2016; published online 22 December 2016)

We perform micromagnetic simulations on the switching of magnetic vortex core by using spin-polarized currents through a three-nanocontact geometry. Our simulation results show that the current combination with an appropriate current flow direction destroys the symmetry of the total effective energy of the system so that the vortex core can be easier to excite, resulting in less critical current density and a faster switching process. Besides its fundamental significance, our findings provide an additional route to incorporating magnetic vortex phenomena into data storage devices.

Keywords: magnetic vortex core, polarity switching, spin-polarized current, micromagnetic simulations

PACS: 75.70.Kw, 67.30.hj, 72.25.Ba, 75.40.Mg **DOI:** 10.1088/1674-1056/26/1/017502

1. Introduction

A magnetic vortex stabilized in a micron or submicron sized ferromagnetic structure is a curling magnetization distribution and the magnetization points perpendicularly to the plane with about a 10-nm-sized vortex core (VC) at the center of the platelet.[1,2] The dynamics of magnetic vortex has attracted considerable attention for its extensive applications such as microwave technologies,[3] magnetic memories,[4] and cancer-cell destruction.[5] To trigger vortex dynamics, the researchers prefer spin-polarized current because the current is easier to apply and consumes less energy than a magnetic field. Yamada *et al*.[6] and Liu *et al*.[7] first reported the VC reversal mediated by in-plane ac current and the VC reversal triggered by out-of-plane dc current was first reported by Caputo *et al*.[8] and Liu *et al*.[9] However, a high value of critical current density is the major difficulty in it being used in practice[10] and less switching time of magnetization reversal also has the utmost significance in high density magnetic recording and information processing technology.[11] Researchers have explored many methods to reduce critical current density and switching time, including an asymmetry pinning layer, composite free layer, nanocontact geometry, laser-induced spin dynamics, and seeking new materials.[12–20] Moreover, all kinds of assisted methods, such as microwave field, static magnetic field, alternating magnetic field, and thermal fluctuations were also extensively used in the studies of manipulation of magnetization orientations.[21–23]

In this paper, we present a method to reduce critical current density and switching time by using a three-nanocontact geometry in a confined structure. Recently, many studies about nanocontact geometry have been reported. The one-nanocontact geometry was mainly used to excite the VC oscillations,[24–26] and in the studies of one-nanocontact geometry, the contact usually is placed in the center of the sample, where the VC is difficult to excite because of the symmetry of the total effective energy of the system, and it is the drawback of such a geometry. The common method to solve this problem is to add a biased in-plane field to shift the VC from the center of the nanodisk before applying the perpendicular spin-polarized current.[27,28] Various multi-nanocontact structures have been designed to achieve the independent controllability of each contact experimentally. Moreover, the multi-nanocontact geometry was commonly applied to phase locking of several oscillators for reducing the line width and increasing the power to a practical application level.[29–32] Further studies demonstrated that the magnetization configurations were influenced by distance and the current flow direction of the multi-nanocontact current.[33,34] We found that the trajectory and frequency of VC were also influenced by the current direction and distance.[35,36] These studies inspired us to design a new model to study the VC switching, where the out-of-plane spin-polarized currents are injected through a three-nanocontact geometry with tunable center-to-center distance and different current directions to make a nonuniform system, making it easier to excite the VC to switch with shorter time and less current density.

2. Model and micromagnetic simulations

A permalloy (Py: $Ni_{80}Fe_{20}$) nanodisk of radius R=200 nm and thickness $L = 10$ nm is chosen as the model and its ground state is a vortex with polarity and chirality $(p,c) = (1,1)$, as illustrated in Fig. 1(a). The currents with the same magnitude

*Project supported by the China Postdoctoral Science Foundation (Grant No. 2013M541286), the Science and Technology Planning Project of Jilin Province, China (Grant Nos. 20140520109JH and 20150414003GH), and the "Twelfth Five year" Scientific and Technological Research Project of Department of Education of Jilin Province, China.

†Corresponding author. E-mail: huazhongnan@126.com

© 2017 Chinese Physical Society and IOP Publishing Ltd

are applied perpendicularly to the nanodisk through three independent nanocontacts, and the radii of the three contacts are $R_c = 50$ nm, where the spin polarizations of the currents are all assumed to be $S_p = -1$, pointing to the $-z$ direction. The contacts are located on the x axis of the disk symmetrically and their center-to-center distance d is first fixed to be 125 nm. The direction of the applied current is defined as $i_p = +1(-1)$, corresponding to the $+z$ $(-z)$ direction. Accordingly, we choose $(i_{p1}, i_{p0}, i_{p2}) = (1,1,1)$, $(i_{p1}, i_{p0}, i_{p2}) = (1,1,-1)$ and $(i_{p1}, i_{p0}, i_{p2}) = (-1,1,-1)$ to study the vortex polarity reversal, the subscripts p0, p1, and p2 indicate the current located in the center of the disk and the other two currents are in the x axis, respectively.

The magnetization dynamics of VC is calculated by the Object Oriented Micromagnetic Framework (OOMMF) code, which is based on the Laudau–liftshitz–Gilbert equation extended by the Slonczewski spin-transfer torque.[37,38] The spin-transfer torque term is expressed as $T_{STT} = \gamma\beta \boldsymbol{m} \times (\boldsymbol{m} \times \boldsymbol{m}_P)$, $\beta = \frac{h}{2\pi} PJ/(2\mu_0 M_S L)$ where $\boldsymbol{m}_P$ is the unit vector of the spin polarization direction, γ the gyromagnetic ratio, h Plank's constant, P the degree of spin polarization, J the current density, μ_0 the vacuum permeability, e the electron charge, and M_S the saturation magnetization. In the simulations, the cell size is $2.5\times2.5\times10$ nm^3 and the magnetic parameters used for Py are as follows: $P = 0.4$, $M_s = 8.6\times10^5$ A/m, the exchange constant $A = 1.3\times10^{-11}$ J/m, and the Gilbert damping parameter $\alpha = 0.05$. In this study, both the spin-transfer torque of spin-polarized current acting directly on the vortex and comparable Oersted field accompanying the current are taken into consideration, where the Oersted field is calculated by using the Biot–Savart law.

3. Results and discussion

Figure 1(b) shows the critical current density (J_c) and the corresponding switching time (T_s) for three current combinations. For comparison, we also perform the micromagnetic simulations of magnetization dynamics excited by one nanocontact with the same contact radius R_c=50 nm, and J_c and T_s are also illustrated in Fig. 1(b). We find that the VC in one-nanocontact geometry can be switched at $J_c = 16\times10^{11}$ A/m^2 and $T_s = 19.7$ ns. However, critical current density and switching time change greatly for three combinations. For $(i_{p1}, i_{p0}, i_{p2}) = (1,1,1)$, $J_c = 6\times10^{11}$ A/m^2, and $T_s = 42.8$ ns, the critical current density decreases by over 50% compared with the case of one nanocontact, whereas the switching time of VC is relatively long. For $(i_{p1}, i_{p0}, i_{p2}) = (-1,1,-1)$, T_s is almost the same as that of the one-nanocontact case, however, the critical current density decreases to $J_c = 12\times10^{11}$ A/m^2. We find the exciting results for both critical current density and switching time in the current combinations $(i_{p1}, i_{p0}, i_{p2}) = (1,1,-1)$. The critical current density decreases to $J_c = 6\times10^{11}$ A/m^2 and T_s is only 3.88 ns, indicating that the VC completes the reversal in a very short time with very low current density. In addition, the magnitudes of J_c and T_s are also dominant compared with the minimum critical switching current density $J_c = 8\times10^{11}$ A/m^2 and its corresponding switching time $T_s = 7.83$ ns in a confined off-centered geometry.[20]

To explain the changes of switching time and critical current density, we first need to clarify the specific switching mechanism of VC in this model system. The simulations reveal that the switching of VC is through the nucleation and subsequent annihilation of vortex–antivortex pair. In order to clarify the VC switching process of this mechanism, we illustrate the in-plane and out-of-plane magnetization changes in the VC switching process as shown in Fig. 2. Figure 2(a) shows the initial state of VC. Owing to the influence of the current, the initial core is slightly displaced from the center and undergoes a counterclockwise spiral motion as shown in Fig. 2(b). For a large displacement, the circular symmetric distribution of the in-plane magnetization around the core is deformed, and then a new vortex-antivortex pair with opposite polarities forms on the inner side of the initial vortex (see Fig. 2(c)). The new antivortex annihilates with the initial vortex shown in Fig. 2(d), the vortex with the negative polarity remains there, and the core switching process is

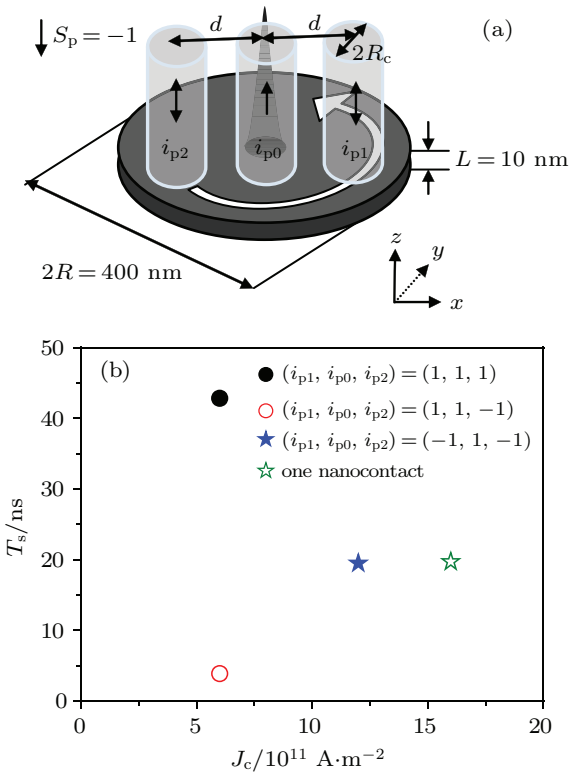


Fig. 1. (color online) (a) Schematic illustration of the model system. The polarized currents are applied via three nanocontacts represented by white cylinders with radius R_c. The radius of the Permalloy dot is $R = 200$ nm and its thickness is $L = 10$ nm. The magnetization distributions are indicated by the out-of-plane cone and the white arrow, respectively. (b) Critical current density and the corresponding switching time of different current combinations as noted and one nanocontact.

completed as shown in Fig. 2(e). The gyroforce is responsible for the VC excitation and Guslienko *et al.* explored the physical origin through analytical and micromagnetic calculations, and their calculation results reveal that the vortex core reversal originates from a gyrotropic field, which is induced by the vortex dynamic motion and is proportional to the velocity of the moving vortex.[39] This switching mechanism is similar to that in the nanodisk in which the vortex polarity switching has been reported by applying various magnetic fields or in-plane currents.[7,20,39–42]

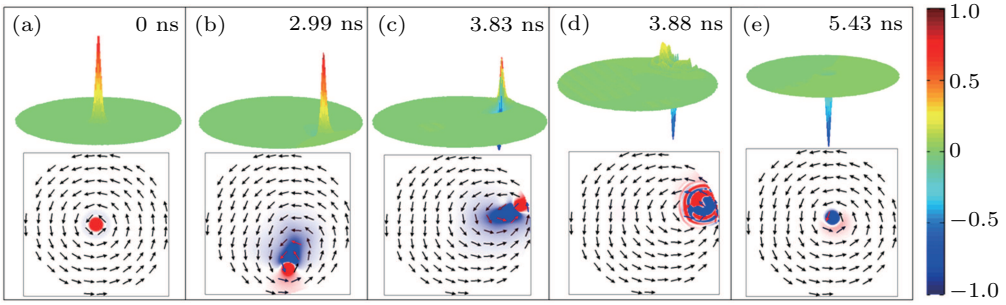


Fig. 2. (color online) Process of vortex core switching of current combinations $(i_{p1}, i_{p0}, i_{p2}) = (1, 1, -1)$ at $J = 6 \times 10^{11}$ A/m^2.

While the discussion above shows the changes of magnetization in the process of VC switching, another vital problem is the changes of velocity and trajectory during the VC switching. The nucleation and annihilation of the vortex-antivortex pair reversal mechanism require the VC to reach the critical switching velocity, and its value for Py is 320–370 m/s,[43] so we plot the velocity and trajectory versus time at the corresponding critical current density for each of three current combinations shown in Fig. 3 to analyze their differences. We find from the simulation that the critical switching velocity for the VC here is 350 m/s, and the velocities and trajectories for three current combination cases are also different. Note that the VC is not excited at first, it stays in the center of the nanodisk for several nanoseconds after the current was applied for $(i_{p1}, i_{p0}, i_{p2}) = (1,1,1)$ and $(i_{p1}, i_{p0}, i_{p2}) = (-1,1,-1)$, leading to the relatively long switching time. However, the VC is excited immediately after the current has been applied for $(i_{p1}, i_{p0}, i_{p2}) = (1,1,-1)$ and the VC reaches the critical switching velocity in a very short time, resulting in a faster switching process (see Fig. 3(b)). Through the analyses on the velocities of three combinations, we find that the VC spends less time to depart from its equilibrium position at current combinations $(i_{p1}, i_{p0}, i_{p2}) = (1,1,-1)$, resulting in faster VC switching, whose physics origin will be analyzed in detail in Fig. 4. For trajectory, the VC experiences spiral motion till switching. However, it should be stressed that the trajectory of VC is obviously distinct from the previously observed circular trajectory for the case of one nanocontact.[28] In our model, the trajectory is obviously affected by the direction of current. For $(i_{p1}, i_{p0}, i_{p2}) = (1,1,1)$ and $(i_{p1}, i_{p0}, i_{p2}) = (-1,1,-1)$, the orbits are elongated or compressed along the x axis, while its equilibrium position is still in the center of the nanodisk. However, the orbit of VC is not a circle anymore for $(i_{p1}, i_{p0}, i_{p2}) = (1,1,-1)$ and its equilibrium also changes, because, we find, the VC after reversal does not return to the center of the nanodisk but stays at the right position of the x axis in the nanodisk, which means that the equilibrium position of the system is shifted for this current combination.

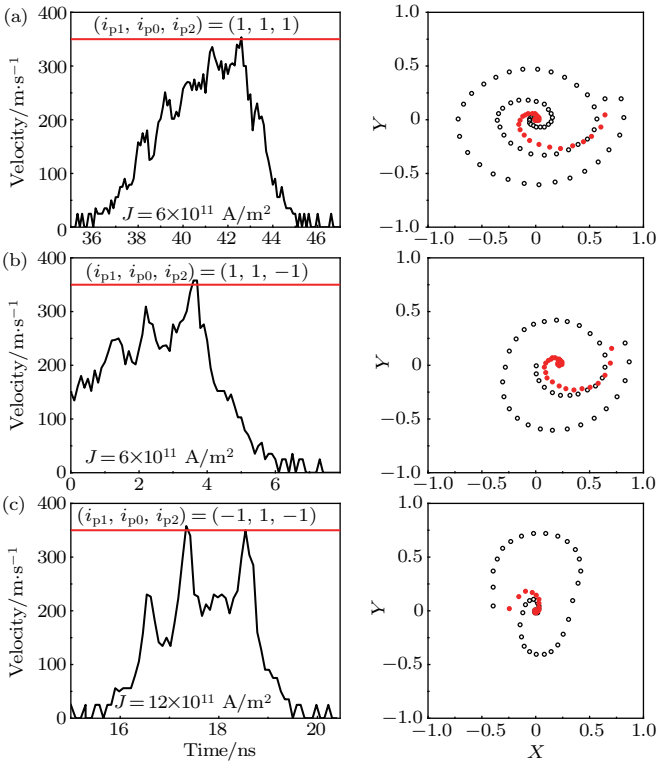


Fig. 3. (color online) Plots of velocity and trajectory of vortex core at the corresponding critical current density for three current combinations ((a) for $(i_{p1}, i_{p0}, i_{p2}) = (1,1,1)$, (b) for $(i_{p1}, i_{p0}, i_{p2}) = (1,1,-1)$ and (c) for $(i_{p1}, i_{p0}, i_{p2}) = (-1,1,-1)$). The red line denotes the critical velocity of vortex core switching, its value is 350 m/s, and the black empty circles and red solid circles represent the trajectories before and after switching, respectively.

As the next step, we will explain the reason for the shorter switching time and the equilibrium shifts in $(i_{p1}, i_{p0}, i_{p2}) = (1,1,-1)$. We notice that the trajectory shown in Fig. 3(b) is an off-centered trace and its gyration center is not the center of the nanodisk, indicating that the equilibrium of the VC motion changes. To elucidate the shifts of the equilibrium, we need to calculate the total effective potential energy

of the model system. The magnetostatic energy due to the core displacement and the Oersted field energy resulting from the applied current constitute the total effective potential energy of the system, here we ignore the exchange energy because it is very low in our model system. The magnetostatic energy can be calculated by $W_{\rm m} = \kappa_0 |\boldsymbol{X}_0|^2/2$, where stiffness coefficient $\kappa_0 = 10/9(M_{\rm S}^2 L^2/R)$, $|\boldsymbol{X}_0|$ is the distance between the VC and the center of the nanodisk center. The Oersted magnetic energy is calculated with $W_n = -\int \boldsymbol{M}\cdot\boldsymbol{H}_n {\rm d}V$ $(n = 0,1,2)$, where $\boldsymbol{H}_n$ are the Oersted fields generated by three currents in the disk plane, respectively. Figure 4 shows the distributions of the total effective potential energy for three current combinations. We find that none of the total effective potential energies is circularly symmetric for three current combinations. The total energies are both bilaterally symmetric for current combinations $(i_{\rm p1}, i_{\rm p0}, i_{\rm p2}) = (1,1,1)$ and $(i_{\rm p1}, i_{\rm p0}, i_{\rm p2}) = (-1,1,-1)$ as shown in Figs. 4(a) and 4(c), and the minimum energies are both in the center of the nanodisk, so none of their equilibrium positions is shifted. However, the total energy is not symmetric for $(i_{\rm p1}, i_{\rm p0}, i_{\rm p2}) = (1,1,-1)$ shown in Fig. 4(b) and the minimum energy of the system is shifted to some position on the $+x$ axis, so the equilibrium position is not in the center of the nanodisk anymore but should be in the position where the total potential effective energy is minimum. The VC will rotate back to this position after reversal, thus the VC stays at this position of the $+x$ axis.

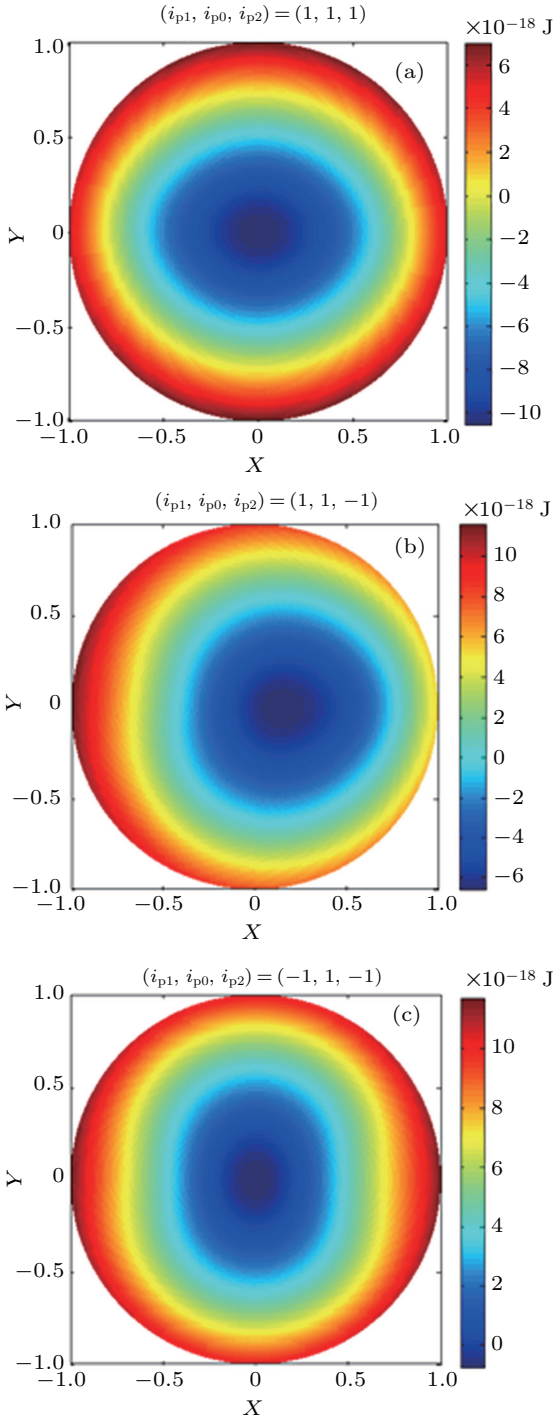


Fig. 4. (color online) Distributions of total effective potential energy for (a) $(i_{\rm p1}, i_{\rm p0}, i_{\rm p2}) = (1,1,1)$, (b) $(i_{\rm p1}, i_{\rm p0}, i_{\rm p2}) = (1,1,-1)$ and (c) $(i_{\rm p1}, i_{\rm p0}, i_{\rm p2}) = (-1,1,-1)$ with the current density being the same as those in Fig. 3.

Actually, we have performed simulations at various center-to-center distances ranging from $d = 100$ nm to $d = 150$ nm in order to find the influences of the nanocontact distance on the critical current density and switching time. Figure 5 shows the critical current density and the corresponding switching time for various d values. For $(i_{\rm p1}, i_{\rm p0}, i_{\rm p2}) = (1,1,-1)$, the switching time and critical current density are both lowest. For $(i_{\rm p1}, i_{\rm p0}, i_{\rm p2}) = (1,1,1)$, the critical current density is relatively low, but the switching time is the longest. For $(i_{\rm p1}, i_{\rm p0}, i_{\rm p2}) = (-1,1,-1)$, the switching time and critical current density are between those of the other two current combinations. For three current combinations, the trends of critical current density and switching time are similar to the scenario of $d = 125$ nm except for the trivial changes of values, indicating that d exerts negligible influence on $J_{\rm c}$ and $T_{\rm s}$.

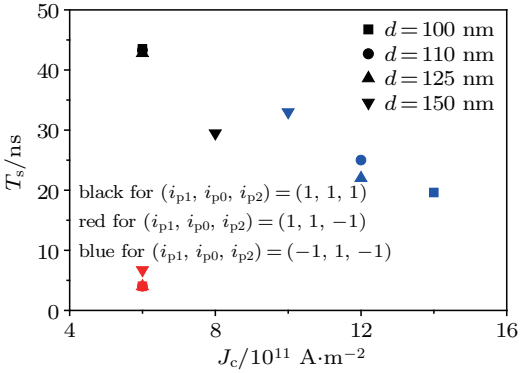


Fig. 5. (color online) Critical current density and the corresponding switching time for various d between the nanocontacts.

4. Conclusions

In conclusion, we realize the faster VC switching with lower current density through breaking the symmetry of the total effective potential energy of the system by using different direction current combinations. The micromagnetic simulations reveal that the switching time and critical current density

are highly sensitive to current direction, but insensitive to the distance between the nanocontacts.

References

[1] Cowburn R P, Koltsov D K, Adeyeye A O, Welland M E and Tricker D M 1999 *Phys. Rev. Lett.* **83** 1042

[2] Shinjo T, Okuno T and Hassdorf R 2000 *Science* **289** 930

[3] Devolder T, Kim J V, Crozat P, Chappert C, Manfrini M, Kampen M, van Roy W, Lagae L, Hrkac G and Schrefl T 2009 *Appl. Phys. Lett.* **95** 012507

[4] Pigeau B, de Loubens G, Klein O, Riegler A, Lochner F, Schmidt G, Molenkamp L W, Tiberkevich V S and Slavin A N 2010 *Appl. Phys. Lett.* **96** 132506

[5] Kim D H, Rozhkova E A, Ulasov I V, Bader S D, Rajh T, Lesniak M S and Novosad V 2010 *Nat. Mater.* **9** 165

[6] Yamada K, Kasai S, Nakatani Y, Kobayashi K, Kohno H, Thiaville A and Ono T 2007 *Nat. Mater.* **6** 270

[7] Liu Y, Gliga S, Hertel R and Schneider C M 2007 *Appl. Phys. Lett.* **91** 112501

[8] Caputo J G, Gaididei Y, Mertens F G and Sheka D D 2007 *Phys. Rev. Lett.* **98** 056604

[9] Liu Y W, He H and Zhang Z Z 2007 *Appl. Phys. Lett.* **91** 242501

[10] Münzenberg M 2010 *Physics* **3** 19

[11] Bedau D, Liu H, Bouzaglou J J, Kent A D and Sun J Z 2010 *Appl. Phys. Lett.* **96** 022514

[12] Li X, Zhang Z Z, Jin Q Y and Liu Y W 2009 *New J. Phys.* **11** 023027

[13] LiuY, Li H N, Hu Y and Du A 2013 *Phys. Status. Solidi B* **250** 1578

[14] You C Y 2012 *Appl. Phys. Lett.* **100** 252413

[15] Lee S C, Pi U H, Kim K, Kim K S, Shin J and Chung U In 2012 *Sci. Rep.* **2** 1

[16] Berkov D V, Boon C T and Krivorotov I N 2011 *Phys. Rev. B* **83** 054420

[17] Vahaplar K, Kalashnikova A M, Kimel A V, Hinzke D and Nowak U 2009 *Phys. Rev. Lett.* **103** 117201

[18] Vomir M, Andrade L H F, Guidoni L, Beaurepaire E and Bigot J Y 2005 *Phys. Rev. Lett.* **94** 237601

[19] Meng H and Wang J P 2006 *Appl. Phys. Lett.* **89** 152509

[20] Li H N, Liu Y, Jia M and Du A 2015 *J. Magn. Magn. Mater.* **386** 8

[21] Wang J B, Mu C P, Wang W W, Zhang B, Xia H Y, Liu Q F and Xue D S 2011 *Appl. Phys. Lett.* **99** 032502

[22] Mu C P, Wang W W, Xia H Y, Zhang B, Liu Q F and Wang J B 2012 *J. Nanosci. Nanotechnol.* **12** 7460

[23] Gliga S, Yan M, Hertel R and Schneider C M 2008 *Phys. Rev. B* **77** 060404

[24] Choi Y S, Lee K S and Kim S K 2009 *Phys. Rev. B* **79** 184424

[25] Mistral Q, Kampen M van, Hrkac G, Kim J V, Devolder T, Crozat P, Chappert C, Lagae L and Schrefl T 2008 *Phys. Rev. Lett.* **100** 257201

[26] Manfrini M, Devolder T, Kim J V, Crozat P, Zerounian N, Chappert C, Roy W Van, Lagae L, Hrkac G and Schrefl T 2009 *Appl. Phys. Lett.* **95** 192507

[27] Aranda G R, Gonzalez J M, del V J J and Guslienko K Y 2010 *J. Appl. Phys.* **108** 123914

[28] Liu Y, Li H N, Hu Y and Du A 2012 *J. Appl. Phys.* **112** 093905

[29] Ruotolo A, Cros V, Georges B, Dussaux A, Grollier J, Deranlot C, Guillemet R, Bouzehouane K, Fusil S and Pert A 2009 *Nat. Nanotechnol.* **4** 528

[30] Kaka S, Pufall M R, Rippard W H, Silva T J, Russek S E and Katine J A 2005 *Nat. Lett.* **437** 389

[31] Mancoff F B, Rizzo N D, Engel B N and Tehrani S 2005 *Nat. Lett.* **437** 393

[32] Manfrini M, Kim J V, Watelot S P, Roy W V, Lagae L, Chappert C and Devolder T 2013 *Nat. Nanotech.* **265** 1

[33] Sani S R, Persson J, Mohseni S M, Fallahi V and Åkerman J 2011 *J. Appl. Phys.* **109** 07C913

[34] Li H N, Liu Y and Du A 2013 *J. Magn. Magn. Mater.* **341** 45

[35] Liu Y, Li H N, Hu Y and Du A 2014 *J. Solid. State. Commun.* **193** 61

[36] Li H N, Liu Y and Du A 2015 *Chin. Phys. B* **24** 047501

[37] Slonczewski J C 1996 *J. Magn. Magn. Mater.* **159** L1

[38] Donahue M J and Porter D G *OOMMF User's Guide*, Version 1.2a5, http://math.nist.gov/oommf/

[39] Guslienko K Yu, Lee K S and Kim S K 2008 *Phys. Rev. Lett.* **100** 027203

[40] Liu Y W, Hou Z W, Gliga S and Hertel R 2009 *Phys. Rev. B* **79** 104435

[41] Lee K S, Guslienko K Y, Lee J Y and Kim S K 2007 *Phys. Rev. B* **76** 174410

[42] Van Waeyenerge B, Puzic A, Stoll H, et al. 2006 *Nat. Lett.* **444** 461

[43] Lee K S, Kim S K, Yu Y S, Choi Y S, Guslienko K Yu, Jung H and Fischer P 2008 *Phys. Rev. Lett.* **101** 267206